CLICdp-Conf-2016-004
25 March 2016

Measurement of the Higgs decay to electroweak bosons at low and intermediate CLIC energies

I. Božović-Jelisavčić[1)]*, G. Milutinović-Dumbelović*, M. Pandurović*, S. Lukić*

On behalf of the CLICdp collaboration

* *Vinca Institute of Nuclear Sciences, University of Belgrade, Serbia*

Abstract

In this paper a simulation of measurements of the Higgs boson decay to electroweak bosons in e^+e^- collisions at CLIC is presented. Higgs boson production and subsequent $H \to ZZ^*$ and $H \to WW^*$ decay processes were simulated alongside the relevant background processes at 350 GeV and 1.4 TeV center-of-mass energy. Full detector simulation and event reconstruction were used under realistic beam conditions. The achievable statistical precision of the measured product of the Higgs production cross section and the branching ratio for the analysed decays has been determined.

Talk presented at International Workshop on Future Linear Colliders (LCWS15), Whistler, Canada, 2-6 November 2015

[1)] ibozovic@vinca.rs

1 Introduction

The future Compact Linear Collider (CLIC) offers excellent potential for a precise and comprehensive set of measurements of the properties of the Higgs boson. Compared to hadron colliders, e^+e^- collider experiments offer an environment of low QCD background, fully reconstructable process kinematics and low radiation levels. The current staged approach to CLIC construction and operation foresees three stages, with 380 GeV, 1.4 TeV and 3 TeV in the center-of-mass (CM), with an integrated luminosity of 500 fb^{-1}, 1.5 ab^{-1} and 3 ab^{-1}, for the three respective energy stages, in order to maximize the physics potential of the experiment in the shortest time. The studies presented in this paper have been carried-out assuming a staging scenario with 350 GeV as the CM energy of the first stage.

Precise exploration of the Higgs properties allows to eventually address physics beyond the Standard Model (SM) through deviations from the SM predicted values. Couplings to electroweak (EW) bosons are of particular interest to probe the Higgs boson structure (i.e. compositeness). In theoretical models extending the SM, the relative deviation of the Higgs couplings w.r.t. the SM is of the order v^2/Λ^2, where v is the vacuum expectation value of the Higgs field and Λ is the scale of the new physics. It follows, e.g., that a 5% deviation can be expected for $\Lambda = 1\,\text{TeV}$. In this context, the measurement precision of the Higgs couplings determines the scale that can be accessed. As discussed in [1, 2], a fit to the full set of data from all energy stages allows extraction of all Higgs couplings with best precision. In particular, the couplings to the vector bosons are determined with a sub-percent uncertainty [1]. It is therefore important to optimize every single measurement for the best achievable statistical precision. The analyses of the measurement of the $H \to ZZ^*$ and $H \to WW^*$ decays presented here focus on the statistical uncertainties of the measured product of the Higgs production cross-section and the corresponding branching fraction.

1.1 Simulation and reconstruction

The analyses were performed using a full simulation of the CLIC_ILD detector concept. The CLIC_ILD concept is derived from the ILD detector proposed for the International Linear Collider [3] and adapted to the CLIC experimental conditions [4].

Event generation for signal and background has been performed with WHIZARD V1.95 [5, 6], using PYTHIA V6.4 [7] to simulate the hadronization processes. Initial state radiation (ISR) and a realistic beam spectrum are included in the simulation using results of the beam-beam simulation with GUINEAPIG 1.4.4 [8]. Equivalent photon approximation (EPA) is used to describe events with virtually exchanged photons below 4 GeV. Hadronic background produced from Beamstrahlung photons has been overlaid to the simulated events before the digitization step. The PANDORAPFA [9, 10] algorithm is employed to ensure particle identification and energy determination. The IsolatedLeptonFinder [11] and TauFinder [12] MARLIN processors are used to identify electrons, muons and tau leptons, respectively. The LCFIplus MARLIN processor was used for flavour tagging [13]. Unpolarised beams were assumed, so obtained results are somewhat conservative since the Higgs production cross-section can be enhanced by the beam polarization [1].

2 Higgs decay to a WW* pair at 350 GeV

At the first CLIC energy stage with $\sqrt{s}$ =350 GeV, the leading Higgs production channel is the s-channel Higgsstrahlung process, $e^+e^- \to HZ$. The Higgs decay to a W-pair is studied, where the W bosons decay hadronically, $H \to WW^* \to q\bar{q}q\bar{q}$. The branching fraction for the decay $H \to WW^*$ is 21.5% [14], out of which 45.6% W-pairs decay hadronically [14]. Therefore the signal repersents 9.8% of all Higgs boson decays.

The final states of the HZ system are subdivided according to the Z boson decay into the fully hadronic final state, where the Z boson decays to a pair of jets ($Z \to q\bar{q}$) and the semileptonic final state, where

Table 1: List of considered processes with the corresponding cross-sections at $\sqrt{s} = 350GeV$.

Signal process	$\sigma(fb)$
$e^+e^- \to HZ, H \to WW^* \to q\bar{q}q\bar{q}$	
$Z \to e^+e^-$	0.453
$Z \to \mu^+\mu^-$	0.454
$Z \to q\bar{q}$	9.16
Background	
$e^+e^- \to HZ$, other Higgs decays	92
$e^+e^- \to q\bar{q}q\bar{q}$	5850
$e^+e^- \to q\bar{q}l^+l^-$	1700
$e^+e^- \to q\bar{q}l\nu$	5910
$e^+e^- \to q\bar{q}\nu\bar{\nu}$	325
$e^+e^- \to H\nu_e\bar{\nu}_e$	52
$e^+e^- \to t\bar{t}$	450
$e^+e^- \to W^+W^-Z$	10

the Z decays to a pair of electrons or muons ($Z \to l^+l^-; l = e, \mu$). In Table 1, the list of the signal and the most relevant background processes is given with the corresponding cross sections. Higgs decays to final states other than a WW^* pair were included as background.

2.1 Method

Event selection is performed in several steps. First the event type is determined by searching for isolated leptons from the Z decay. The fully hadronic or semileptonic final states are identified as events containing either zero or two isolated leptons, respectively. In the case of a semileptonic final state, the particle flow objects (PFOs) that are assigned to leptons are removed from the event and the rest of the event is clustered into four jets using the k_t clustering algorithm [15]. The hadronic final states are clustered into six jets. To each jet in an event, b and c-tagging probabilities are assigned.

The next step is the identification of the Higgs candidate, one on-shell and one off-shell W boson candidate and the Z boson candidate. For the hadronic final state the best combination of jet pairs is found by minimisation of the total χ^2 of the corresponding boson masses:

$$\chi^2 = \frac{(m_{ij} - m_W)^2}{\sigma^2_{m_W}} + \frac{(m_{kl} - m_Z)^2}{\sigma^2_{m_Z}} + \frac{(m_{ijmn} - m_H)^2}{\sigma^2_{m_H}}, \qquad i,j,k,l,m,n = 1,6 \tag{1}$$

where σ_{m_V} (V = W, Z, H) stands for the measured widths of the corresponding boson invariant mass distributions. For the semileptonic final state, the Z boson is reconstructed using the selected leptons, while the on-shell W boson is reconstructed from the pairs of jets closest to the W mass:

$$(\Delta m_W)_{\min} = \min |m_W - m_{ij}|. \qquad i,j = 1,4 \tag{2}$$

A preselection based on kinematic variables is applied in order to reduce large cross-section background processes. After the preselection, a multivariate analysis (MVA) [16] event selection with the Boosted Decision Tree (BDT) classifier is performed on the basis of kinematic properties of the event, in order to reject the residual background. The expected relative statistical uncertainty of the product of the Higgsstrahlung cross-section and the corresponding branching ratio is calculated as:

$$\delta(\sigma \times BR) = \frac{\sqrt{N_S + N_B}}{N_S}, \tag{3}$$

where N_S and N_B denote the number of selected signal and background events.

2.2 Preselection

Different preselection criteria are applied to different types of final states. For the semileptonic final states the conditions are imposed on the invariant mass of the Z boson (70 GeV < m_Z < 110 GeV) and on the number of the particle flow object $N_{\mathrm{PFO}} > 20$ in order to reduce background from the high cross-section processes $e^+e^- \to q\bar{q}l\nu$ and $e^+e^- \to q\bar{q}l^+l^-$.

For the fully hadronic final state the following criteria were applied to reduce background from the $e^+e^- \to q\bar{q}q\bar{q}$ and $e^+e^- \to q\bar{q}\nu\bar{\nu}$ processes:

- the invariant mass of the Z boson candidate, $m_Z > 40\,\mathrm{GeV}$;
- jet transition probabilities, $-\log y_{12} < 2.0$, $-\log y_{23} < 2.6$, $-\log y_{34} < 3.0$, $-\log y_{45} < 3.2$, $-\log y_{56} < 4.0$;
- visible energy in the event, $E_{\mathrm{vis}} > 250$ GeV;
- number of particle flow objects, $N_{\mathrm{PFO}} > 50$;
- event thrust, thrust < 0.9;
- b-tag probabilities of all jets, $P_{\mathrm{b}}^{\mathrm{jet}_i} < 0.9$.

The signal preselection efficiency is 71% for the fully hadronic final state and 80 and 87% for the semileptonic e^+e^- and $\mu^+\mu^-$ final states, respectively.

2.3 MVA selection

After the preselection, the MVA event selection is applied, optimized for the best statistical precision of $\sigma \times \mathrm{BR}$ (Eq. (3)) with 500 fb^{-1} of collected data. The following observables are used for the classification of events in the analysis of all final states: masses of the on- and off-shell W boson candidates, the Z boson mass and the Higgs mass, jet transition probabilities, the transverse momentum of the Higgs boson jets, b-tag and c-tag probabilities of jets and event shape variables. In addition to these variables, the angle between jets that constitute Z and Higgs boson candidates are used for the selection of the hadronic final state. Similarly, the polar angle of the Z boson is used for the selection of the semileptonic final state.

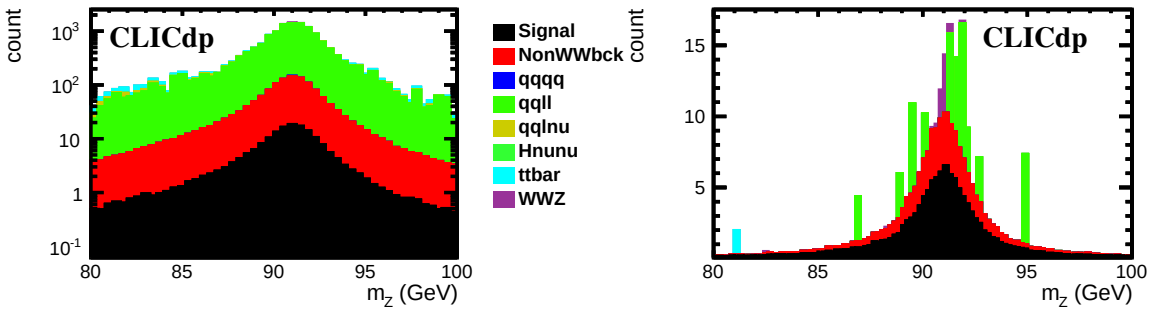

Figure 1: The Z invariant mass distribution after the preselection (left) and after MVA selection (right) for the semileptonic $Z \to \mu^+\mu^-$ final state, assuming 500 fb^{-1} of data.

The corresponding distributions of the Z invariant mass, after preselection and MVA event selection are given in Fig. 1 and Fig. 2, for the semileptonic and the hadronic final states, respectively. After the final selection, the total signal efficiency is 42% and 55%, for the e^+e^- and $\mu^+\mu^-$ final states, respectively. For the fully hadronic final state the overall signal efficiency is 29%.

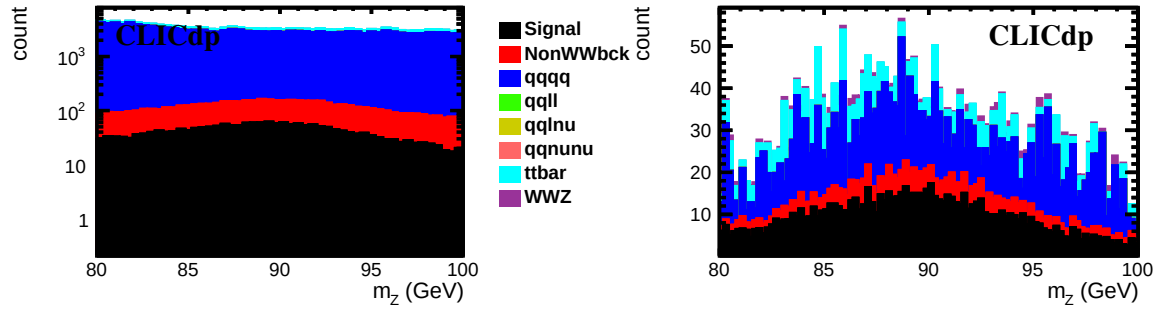

Figure 2: The Z invariant mass distribution after the preselection (left) and after MVA selection (right) for the hadronic ($Z \to q\bar{q}$) final state, assuming 500 fb^{-1} of data.

The expected statistical accuracy for the measurements of $\sigma_{HZ} \times BR_{H\to WW^*}$ is found to be 5.9%, 13.1% and 16.1% for the hadronic, $\mu^+\mu^-$ and e^+e^- final states of the Z boson, respectively. Detailed results for the $\sigma_{HZ} \times BR_{H\to WW^*}$ measurement are listed in Table 2.

Table 2: Summary of the simulation results for the $\sigma_{HZ} \times BR_{H\to WW^*\to q\bar{q}q\bar{q}}$ measurement at $\sqrt{s} = 350\,\text{GeV}$ CLIC with unpolarised beams and 500 fb^{-1} of data. N_S is the number of signal events in the final selection, ε_S represents the overall signal efficiency and $\delta(\sigma \times BR)$ is the relative statistical accuracy of the measured observable.

	$\sigma_{HZ} \times BR_{H\to WW^*\to q\bar{q}q\bar{q}}$		
	$Z \to e^+e^-$	$Z \to \mu^+\mu^-$	$Z \to q\bar{q}$
N_S	95	125	1328
ε_S	42%	55%	29%
$\delta(\sigma \times BR)$	16.1%	13.1%	5.9%

3 Higgs decay to a ZZ* pair at 1.4 TeV

In the WW-fusion process $e^+e^- \to H\nu_e\bar{\nu}_e$ at 1.4 TeV center-of-mass energy, $H \to ZZ^*$ decays can be measured in the fully hadronic ($ZZ^* \to q\bar{q}q\bar{q}$) and in the semileptonic ($ZZ^* \to q\bar{q}l^+l^-; l = e,\mu,\tau$) final states. The experimental signature is 4 jets, or 2 jets and 2 leptons in the final state, respectively. The total invariant mass of the final state should be consistent with m_H and the invariant mass of one pair of jets or of the lepton pair should be consistent with m_Z.

The branching fraction for the decay $H \to ZZ^*$ is 2.89% [14]. The fully hadronic final state of a ZZ^* pair has a branching ratio of 48.9% [14], resulting in an effective cross section of 3.45 fb for the $e^+e^- \to H\nu_e\bar{\nu}_e \to ZZ^*\nu_e\bar{\nu}_e \to q\bar{q}q\bar{q}\nu_e\bar{\nu}_e$ process, while the semileptonic final state of a ZZ^* pair has a branching ratio of 14.1% [14] and the effective cross section for the $e^+e^- \to H\nu_e\bar{\nu}_e \to ZZ^*\nu_e\bar{\nu}_e \to q\bar{q}l^+l^-\nu_e\bar{\nu}_e$ process is 0.995 fb. This results in 5175 and 1492 signal events, respectively, for the hadronic and the semileptonic final states and for an integrated luminosity of 1.5 ab^{-1}. In Table 3, the list of signal and the most relevant background processes is given, with the corresponding cross sections. The main background process, with the same final state particles as the fully hadronic signal final state, is $e^+e^- \to H\nu_e\bar{\nu}_e \to WW^*\nu_e\bar{\nu}_e \to q\bar{q}q\bar{q}\nu_e\bar{\nu}_e$. Other important background processes are $e^\pm\gamma \to q\bar{q}q\bar{q}\nu$, $\gamma\gamma \to q\bar{q}q\bar{q}$ and $e^\pm\gamma \to q\bar{q}q\bar{q}e^\pm$, due to their large cross sections. The latter can be substantially reduced by requiring high-p_T jets, above 80 GeV, at the preselection level. Other background processes can be discriminated from the signal events using a multivariate approach.

Table 3: List of considered processes with the corresponding effective cross-sections at 1.4 TeV.

Signal processes	σ(fb)
$e^+e^- \to H\nu_e\bar{\nu}_e \to ZZ^*\nu_e\bar{\nu}_e \to q\bar{q}q\bar{q}\nu_e\bar{\nu}_e$	3.45
$e^+e^- \to H\nu_e\bar{\nu}_e \to ZZ^*\nu_e\bar{\nu}_e \to q\bar{q}l^+l^-\nu_e\bar{\nu}_e$	0.995
Background	σ(fb)
$e^+e^- \to H\nu_e\bar{\nu}_e \to WW^*\nu_e\bar{\nu}_e \to q\bar{q}q\bar{q}\nu_e\bar{\nu}_e$	27.6
$e^+e^- \to H\nu_e\bar{\nu}_e \to b\bar{b}\nu_e\bar{\nu}_e$	137
$e^+e^- \to q\bar{q}\nu_e\bar{\nu}_e$	788
$e^+e^- \to q\bar{q}l^+l^-$	2730
$\gamma\gamma \to q\bar{q}l^+l^-$	13800
$e^+e^- \to q\bar{q}l\nu$	4310
$e^\pm\gamma \to q\bar{q}q\bar{q}\nu$	338
$\gamma\gamma \to q\bar{q}q\bar{q}$	30200
$e^\pm\gamma \to q\bar{q}q\bar{q}e^\pm$	2890

3.1 Method

For the semileptonic final state, the first step is the search for isolated leptons (electrons, muons or taus). Exactly two leptons are required, otherwise the event is rejected. If two isolated leptons are found, all remaining particles in the event are clustered into two jets using the k_t algorithm. For the hadronic final state, the event is directly clustered by the k_t algorithm into four jets. For both final states, flavour-tagging is performed to reduce the background from the dominant $H \to b\bar{b}$ process.

Preselection based on kinematic variables is applied as described in Sec. 3.2 to reduce the high cross-section background. After the preselection, an MVA event selection based on the BDT classifier is performed to minimize the residual background. The expected statistical accuracy on $\sigma_{H\nu_e\bar{\nu}_e} \times BR_{H\to ZZ^*}$ is calculated as in Eq. (3).

3.2 Preselection

Two leptons and two jets of the semileptonic final state, or 4 jets of the hadronic final state are paired to form the Z boson candidates. Since $m_H < 2m_Z$, one on-shell and one off-shell Z boson are produced in the Higgs decay. Thus, one Z candidate is required to have invariant mass consistent with m_Z (on-shell Z boson), while the second candidate is required to form the off-shell Z boson. The preselection cuts for the fully hadronic final state are:

- mass of the on-shell Z boson: 45 GeV $< m_Z <$ 110 GeV;
- invariant mass of the off-shell Z boson candidate: $m_{Z^*} <$ 65 GeV;
- higgs invariant mass: 90 GeV $< m_H <$ 165 GeV;
- jet transition probabilities: $-\log y_{34} < 3.5$, $-\log y_{23} < 3.0$;
- visible energy: 100 GeV $< E_{vis} <$ 600 GeV;
- missing transverse momentum: $p_T^{miss} >$ 80 GeV;
- b-tag probabilities of all jets: $P_b^{jet_i} < 0.95$.

For the semileptonic final state, the only preselection criterion is that exactly two isolated leptons are found. The signal preselection efficiency is 32% for the fully hadronic final state and 62% for the

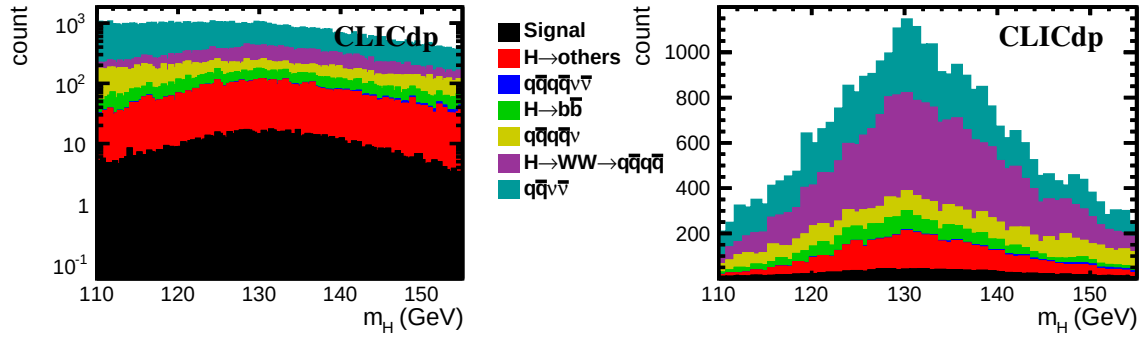

Figure 3: Stacked histograms of the Higgs invariant mass distributions with preselection only (left) and after MVA selection (right) for the fully hadronic final state with 1.5 ab^{-1} of data.

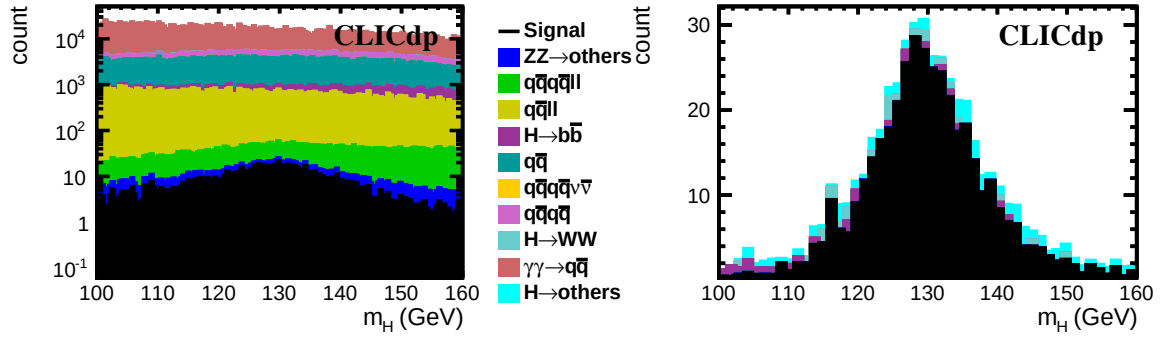

Figure 4: Stacked histograms of the Higgs invariant mass distributions with preselection only (left) and after MVA selection (right) for the semileptonic final state with 1.5 ab^{-1} of data.

semileptonic final state. Only 0.8% of the four-jet backround events $e^{\pm}\gamma \to q\bar{q}q\bar{q}\nu$, $\gamma\gamma \to q\bar{q}q\bar{q}$ and $e^{\pm}\gamma \to q\bar{q}q\bar{q}e^{\pm}$ remain after the preselection. Yet, these background still dominate over the signal due to the large cross-sections (see Fig. 3 left).

3.3 MVA event selection

For the fully hadronic final state, 11 sensitive observables are used for the classification of events: masses of the on- and off-shell Z bosons, the Higgs mass, jet transition probabilities, visible energy, missing transverse momentum, b-tag and c-tag probabilities of the jets. For the semileptonic final state 17 observables are used: masses of the on- and off-shell Z bosons, invariant masses of the dijet and dilepton systems, the Higgs mass, jet transition probabilities, visible energy in the event, the difference between the visible energy in the event and the Higgs visible energy, missing transverse momentum, b-tag and c-tag probabilities of the jets, polar angle of the Higgs candidate and the number of all PFOs in the event.

In both final states, the BDT cut minimizing the statistical uncertainty is chosen (Eq. (3)), giving an overall efficiency of 20% and 28%, for the fully hadronic and semileptonic final states, respectively. The Higgs invariant mass distribution in the fully hadronic events that have passed the preselection is given in Fig. 3 (left), while Fig. 3 (right) shows the same distribution for events passing the BDT selection. The equivalent distributions are shown for the semileptonic final state in Fig. 4.

Statistical uncertainties of $\sigma_{H\nu_e\bar{\nu}_e} \times BR_{H\to ZZ^*}$, derived from Eq. (3), are presented in Table 4 for both final states.

Table 4: Summary of the simulation results for the $\sigma_{H\nu_e\bar{\nu}_e} \times BR_{H\to ZZ^*}$ measurement at 1.4 TeV CLIC with unpolarised beams and for an integrated luminosity of 1.5 ab^{-1}. N_S is the number of selected signal events, ε_S represents the overall signal efficiency and $\delta(\sigma \times BR)$ is the relative statistical accuracy of the measured observable.

	$\sigma_{H\nu_e\bar{\nu}_e} \times BR_{H\to ZZ^*}$	
	$ZZ^* \to q\bar{q}q\bar{q}$	$ZZ^* \to q\bar{q}l^+l^-$
N_S	1031	425
ε_S	20%	28%
$\delta(\sigma \times BR)$	17.7%	5.6%

4 Summary

Detailed analyses of Higgs decays to EW bosons are simulated at low and intermediate CLIC energies. Each analysis is optimized for the best statistical uncertainty.

The product of the Higgsstrahlung cross section and the branching ratio for the decay to a pair of W bosons, $\sigma_{HZ} \times BR_{H\to WW^*}$, is measured at the 350 GeV CM energy with 500 fb^{-1} integrated luminosity, by counting events with fully hadronic decays of W and hadronic and leptonic Z decays. The relative statistical accuracies are 5.9% for the hadronic Z final state and 13.1%, 16.1% for Z decays into muons and electrons, respectively.

The product of the Higgs production cross section in W^+W^- fusion and the branching ratio for the decay to a pair of Z bosons, $\sigma_{H\nu_e\bar{\nu}_e} \times BR_{H\to ZZ}$, is measured at 1.4 TeV CM energy and for 1.5 ab^{-1} integrated luminosity by counting hadronic and semileptonic Z decays. The relative statistical accuracies are 5.6% and 17.7% for the semileptonic and the hadronic final states, respectively.

In both analyses, the statistical uncertainty is dominated by the irreducible background processes and the limited number of signal events in the experiment.

The results of the measurements presented here form part of the complete set of data from all CLIC energy stages used in a global fit to enable determination of the Higgs couplings with the ultimate precision. The couplings to the EW bosons are obtained at a percent or sub-percent level from the model-independent and the model-dependent fits, respectively [1, 2].

References

[1] H. Abramowicz et al.,
Physics at the CLIC e^+e^- Linear Collider – Input to the Snowmass process 2013 (2013), arXiv:1307.5288.

[2] I. Bozovic-Jelisavcic, *CLIC physics overview*, Proceedings of the 17th Lomonosov Conference on Elementary Particle Physics, Moscow, 20 - 26 August, 2015,
URL: http://www.icas.ru/english/LomCon/17lomcon/17lomcon_main.htm.

[3] T. Abe et al., *The International Large Detector: Letter of Intent*, arXiv:1006.3396, 2010.

[4] L. Linssen et al., eds., *Physics and Detectors at CLIC: CLIC Conceptual Design Report*, ANL-HEP-TR-12-01, CERN-2012-003, DESY 12-008, KEK Report 2011-7, arXiv:1202.5940, CERN, 2012.

[5] W. Kilian, T. Ohl, J. Reuter, *WHIZARD: Simulating Multi-Particle Processes at LHC and ILC*, Eur.Phys.J **C71**, 1742 (2011), arXiv:0708.4233.

[6] M. Moretti, T. Ohl, J. Reuter, *O'Mega: An optimizing matrix element generator*, arXiv:hep-ph/0102195, 2001.

[7] T. Sjostrand, S. Mrenna, P. Z. Skands, *PYTHIA 6.4 Physics and Manual*, JHEP **05**, 026 (2006), arXiv:hep-ph/0603175, DOI: 10.1088/1126-6708/2006/05/026.

[8] D. Schulte, *Beam-beam simulations with GUINEA-PIG*, CERN-PS-99-014-LP, 1999.

[9] M. A. Thomson, *Particle Flow Calorimetry and the PandoraPFA Algorithm*, Nucl. Instrum. Methods **A611**, 25 (2009), arXiv:0907.3577, DOI: 10.1016/j.nima.2009.09.009.

[10] J. Marshall, A. Münnich, M. Thomson, *Performance of Particle Flow Calorimetry at CLIC*, Nucl. Instrum. Methods **A700**, 153 (2013), arXiv:1209.4039, ISSN: 0168-9002, DOI: 10.1016/j.nima.2012.10.038.

[11] F. Gaede, J. Engels, *Marlin et al - A Software Framework for ILC detector R&D*, EUDET-Report 2007-11, 2007, URL: http://www.eudet.org/e26/e27/e584/eudet-report-2007-11.pdf.

[12] A. Munnich, *TauFinder: A reconstruction algorithm for tau leptons at linear colliders*, LCD-Note2010-009, 2010, URL: http://cds.cern.ch/record/1443551/files/LCD-2010-009.pdf.

[13] *LCFIPlus*, URL: https://confluence.slac.stanford.edu/display/ilc/LCFIPlus.

[14] S. Dittmaier et al., *Handbook of LHC Higgs Cross Sections: 2. Differential Distributions*, arXiv:1201.3084, 2012.

[15] S. Catani et al., *Longitudinally invariant Kt clustering algorithms for hadron hadron collisions*, Nucl. Phys. B **406**, 187 (1993), URL: http://cds.cern.ch/record/246812/.

[16] A. Hoecker et al., *TMVA - Toolkit for Multivariate Data Analysis*, POSACAT **040** (2007), arXiv:physics/0703039.